JCTC Journal of Chemical Theory and Computation

Reactivities of Sites on (5,5) Single-Walled Carbon Nanotubes with and without a Stone-Wales Defect

T. C. Dinadayalane,[†] Jane S. Murray,[‡] Monica C. Concha,[‡] Peter Politzer,*[,‡] and Jerzy Leszczynski*[,†]

Interdisciplinary Center for Nanotoxicity (ICN), Department of Chemistry and Biochemistry, Jackson State University, 1400 JR Lynch Street, Jackson, Mississippi 39217, and Department of Chemistry, University of New Orleans, New Orleans, Louisiana 70148

Received December 14, 2009

Abstract: The reactivities of various carbon sites on (5,5) single-walled carbon nanotubes (SWCNT) of $C_{70}H_{20}$ with and without a Stone-Wales defect have been predicted computationally. The properties determined include the average local ionization energy $\bar{I}_S(\mathbf{r})$ and pyramidalization angle θ_P on the surfaces of the bare tubes, the chemisorption energies, bond lengths, stretching frequencies for chemisorbed H and F atoms, and the effects of H and F chemisorption upon the HOMO−LUMO energy gaps. There is a good correlation between the minima of the local ionization energy and the chemisorption energies at different carbon sites, indicating that $\bar{I}_S(\mathbf{r})$ provides an effective means for rapidly and inexpensively assessing the relative reactivities of the carbon sites of SWCNTs. The pyramidalization angle (θ_P), which is a measure of local curvature, also shows a relationship to site reactivity. The most reactive carbon site, identified by having the lowest $\bar{I}_S(\mathbf{r})$ and largest θ_P, is in the Stone-Wales defect region, which also has the least reactive carbon site, having the highest $\bar{I}_S(\mathbf{r})$ and smallest θ_P. The presence of a Stone-Wales defect and also by H and F chemisorption decreased the HOMO−LUMO gap of (5,5) SWCNT.

Introduction

Linear single-walled carbon nanotubes (SWCNTs), which can be viewed as wrapped-around graphene sheets, are of interest due to their remarkable electrical, mechanical, optical, and chemical properties.[1−4] Insertion of impurities such as ions, metal atoms, and molecules into SWCNTs modifies their band gaps.[5−7] Introducing defects such as Stone-Wales, vacancies, ad-dimers, etc. opens new opportunities for tailoring the electronic properties of SWCNTs.[8−11] Thus, the defect-containing systems and their functionalized forms could be useful for novel applications. Shigekawa and co-workers have demonstrated the creation and destruction of point defects in SWCNTs using scanning tunneling microscopy (STM). This provides a way to precisely control the electronic properties of SWCNTs.[12]

An important nanotube defect is the Stone-Wales defect, which involves four carbon hexagons being replaced by two pentagons and two heptagons coupled in pairs (5−7−7−5; compare **1** and **2** in Figure 1). The Stone-Wales defect is generated by a 90° rotation of a C−C bond in the hexagonal network.[8] The Stone-Wales transformation has an energy barrier of 6−7 eV in a flat graphene sheet and in C_{60}.[13−16] Suenaga et al. have shown the first direct imaging of pentagon−heptagon pair defects in a SWCNT by means of high-resolution transmission electron microscopy (HR-TEM) with atomic sensitivity.[17] In-depth theoretical studies of Stone-Wales defects in carbon nanotubes are limited. However, some recent ones have shown the Stone-Wales defect in two different orientations, and its influence on covalent and noncovalent functionalization in selected carbon nanotubes.[18−27] The formation of Stone-Wales defects in the catalytically assisted growth mechanism of SWCNTs has been reported by Charlier et al. using *ab initio* molecular dynamics and tight-binding Monte Carlo simulations.[28]

* Corresponding author e-mail: jerzy@icnanotox.org (J.L.); ppolitzer@uno.edu (P.P.).

[†] Jackson State University.

[‡] University of New Orleans.

10.1021/ct900669t
Published on Web 03/10/2010

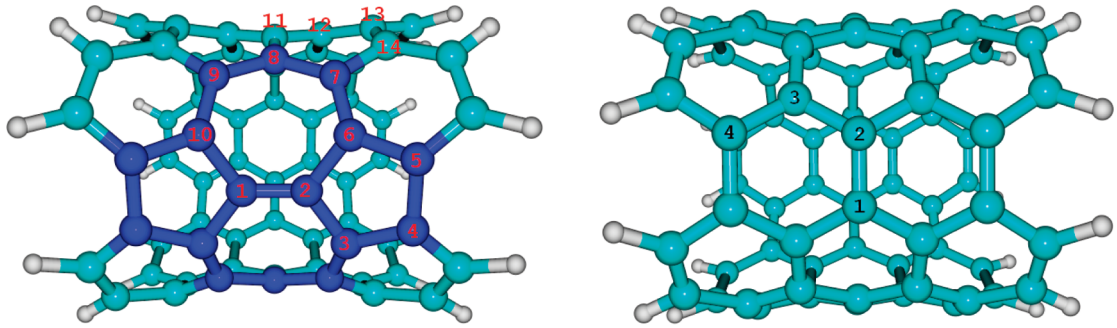

1 **2**

Figure 1. Stone-Wales defect (**1**) and defect-free (**2**) armchair (5,5) SWCNTs, $C_{70}H_{20}$. Atom numberings are indicated. The carbon atoms of the Stone-Wales defect region of **1** are shown in blue for clarity.

Pentagon−heptagon pair defects have been observed experimentally and have been reported to play a crucial role in the growth of the nanotube structure.[28] Robinson et al. demonstrated that the chemical sensitivities of SWCNTs can be enhanced significantly by introducing a low density of defects on their sidewalls.[27] Other theoretical studies showed how the defects participate in the chemical sensing behavior of SWCNTs.[25,26,29]

Defect-free SWCNTs, in general, possess few dissimilar carbon atom sites for attachment of functional groups. In contrast, defect-containing tubes have many different sites with varying reactivities, particularly in the region of the defect. Furthermore, the presence of defects changes the local curvatures of SWCNTs, making the carbon atoms in the vicinity of a defect more or less reactive than in the defect-free region or in the pristine tube. Considering the large sizes of nanotubes, it is important to identify and rank the most reactive sites in defect-containing tubes without performing expensive *ab initio* or DFT calculations.

Hydrogen atom chemisorption on the surfaces of SWCNTs has been the subject of both experimental and theoretical studies, since SWCNTs are viewed as a potential means for hydrogen storage.[30−36] Experimental studies by Nikitin et al. on the hydrogenation of SWCNTs with atomic hydrogen showed that it creates C−H bonds, and these C−H bonds can be completely broken by heating to 600 °C.[30] It was reported that hydrogenation of SWCNTs by H-plasma treatment is useful to cut smaller diameter tubes more easily than larger ones.[31] Lu et al. found that chemisorption of H atoms on the exterior surface of the smaller armchair SWCNTs can break the C−C bonds but does not induce unzipping in larger armchair and zigzag SWCNTs.[37] Recently, Stojkovic et al. demonstrated bisection of SWCNT by controlled chemisorption of hydrogen atoms.[32]

Fluorine chemisorption on the surfaces of SWCNTs has evoked experimental interest because fluorine atoms on nanotubes behave as leaving groups and can be readily replaced by nucleophilic agents.[38] Fluorinated nanotubes were characterized by X-ray diffraction and by X-ray photoelectron and Raman spectroscopy.[39] Fluorination followed by pyrolysis of SWCNTs was reported to have "cut" SWCNTs of a range of different lengths.[40] Chemisorption of fluorine atoms on the external surfaces of defect-free SWCNTs has been investigated by various groups,[41−45] but there are no studies involving defect-containing SWCNTs.

One of the objectives of this work has been to examine the reactivities of different carbon atoms in (5,5) armchair SWCNTs with and without the Stone-Wales defect, using the computed average local ionization energy $\bar{I}(\mathbf{r})$, which will be discussed in the next section. The differing reactivities of the carbon atoms will also be analyzed via chemisorptions of H and F atoms on the external surfaces of the tubes.

The Average Local Ionization Energy

For predicting and interpreting chemical reactivity, which is a local phenomenon that varies from one site to another within a given system, it is essential to have a measure of how readily available, i.e., how strongly held, the electrons are at different sites. It is for this purpose that the average local ionizaton energy, $\bar{I}(\mathbf{r})$, was introduced.[46]

$$\bar{I}(\mathbf{r}) = \frac{\sum_i \rho_i(\mathbf{r})|\varepsilon_i|}{\rho(\mathbf{r})} \tag{1}$$

In eq 1, $\rho_i(\mathbf{r})$ is the electronic density of orbital i, having energy ε_i; $\rho(\mathbf{r})$ is the total electronic density; the summation is over all occupied orbitals.

Within the Hartree−Fock framework, the formalism of the theory plus Koopmans' theorem[47,48] provide support for the approximation $I_i \approx -\varepsilon_i$, where I_i is the ionization energy of the ith electron; in density functional theory, Janak's theorem does the same.[49] Thus, $\bar{I}(\mathbf{r})$ can be regarded as the average energy required to remove an electron from the point $\mathbf{r}$, the focus being upon the point in space rather than a particular orbital.

While our present interest in $\bar{I}(\mathbf{r})$ is primarily as a guide to reactivity, its significance is more far-reaching. $\bar{I}(\mathbf{r})$ is linked to electronegativity, local kinetic energy density, and local polarizability and hardness. These aspects of it are discussed elsewhere.[50,51]

For interpreting and predicting the reactive behavior of a system, $\bar{I}(\mathbf{r})$ is usually computed on its surface and labeled $\bar{I}_s(\mathbf{r})$. The surface is typically taken to be the 0.001 au (electrons/bohr^3) contour of the electronic density $\rho(\mathbf{r})$, as proposed by Bader et al.[52] The local minima of $\bar{I}_S(\mathbf{r})$, designated by $\bar{I}_{S,min}$, indicate the locations of the least tightly held, most reactive electrons. These are accordingly the preferred sites for electrophilic or radical attack. $\bar{I}(\mathbf{r})$ has indeed proven to be quite effective in analyzing reactive

behavior;[46,53−58] for example, it correctly predicts the *ortho*/*para vs*. *meta* directing tendencies of benzene substituents, as well as their activation or deactivation of the ring.[46,54] $\bar{I}(\mathbf{r})$ has been utilized for characterizing graphene[55] and nanotube surfaces.[4,59]

Computational Details

B3LYP/6-31G(d) geometry optimizations were carried out for (5,5) armchair SWCNTs comprised of 70 carbon atoms, both with and without Stone-Wales defects (**1** and **2** in Figure 1). Both ends of the tubes were capped by hydrogen atoms to avoid dangling bonds. The B3LYP/6-31G(d) optimized structures were used to compute the average local ionization energy $\bar{I}_s(\mathbf{r})$ via eq 1 over grids covering both the inner and outer 0.001 au surfaces of the tubes. Due to their large sizes, $\bar{I}(\mathbf{r})$ was calculated at the HF/STO-5G level, which has been found to be quite satisfactory for carbon framework systems.[53,56] For the (5,5) SWCNTs with hydrogen and fluorine atoms bonded at various sites, geometries were optimized and reaction (chemisorption) energies determined with the UB3LYP/6-31G(d) procedure. Vibrational frequency calculations confirmed that all structures correspond to energy minima. All geometry optimizations and frequency calculations were carried out with the Gaussian 03 suite of programs.[60] $\bar{I}_s(\mathbf{r})$ was computed using the HardSurf code.[61]

The numbering of the carbons of tubes **1** and **2** is shown in Figure 1. It should be noted that many sites in each tube are identical by symmetry. For example, C3 in **1** has three identical counterparts. Whatever is said about a particular carbon in the following discussion should be recognized as applying as well to all of its counterparts by symmetry.

Results and Discussion

Figures 2 and 3 depict the average local ionization energies $\bar{I}_s(\mathbf{r})$ on the outer surfaces of the bare (5,5) SWCNTs **1** and **2**. Table 1 lists the local minima, $\bar{I}_{S,min}$, at various carbon atoms. Both the highest and the lowest $\bar{I}_{S,min}$ are in the defect region of **1**. The lowest $\bar{I}_{S,min}$, predicted to indicate the most reactive carbon, is for C3, which is simultaneously part of five-, six-, and seven-membered rings. The carbon atoms C1 and C2, which form the bond sharing two heptagons, have higher $\bar{I}_{S,min}$ than any other carbons in either the defect-containing (**1**) or the defect-free (**2**) SWCNTs. In **1**, the opposite side of the defect exhibits an $\bar{I}_s(\mathbf{r})$ pattern very similar to that of the defect-free tube **2**; compare Figures 2b and 3.

Table 1 also contains the C−H and C−F bond lengths and the reaction energies (ΔE) for the chemisorption of hydrogen and fluorine atoms at the different carbon sites on the outer sides of **1** and **2**. Each chemisorption is computed to be viable; the F atom chemisorption is more favorable (by 10−12 kcal/mol) than the H atom chemisorption at the corresponding carbon atom site. The C−H distances are all about 1.11 Å, close to the 1.09−1.10 Å that is typical of sp^3 carbon,[62] even though the chemisorption energies range from −32.1 to −49.7 kcal/mol. The C−F bond distances are more variable, 1.415 to 1.449 Å, slightly larger than the typical 1.39−1.43 Å.[62] The shortest C−H and C−F bonds and the largest chemisorption energies are at C3 and C14 of **1**. C3 is part of the defect, and C14 adjoins it (Figure 1). In general, Table 1 shows that some of the carbon atoms in the defect

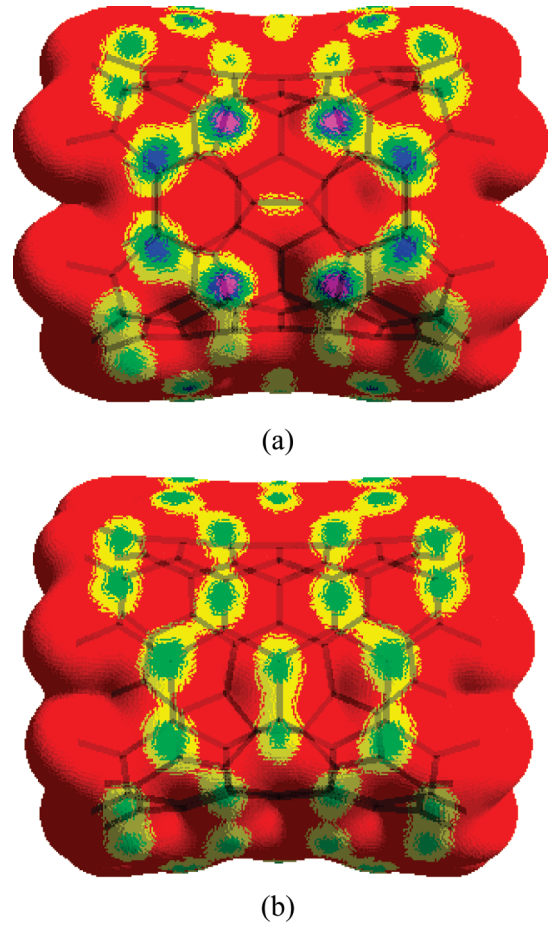

Figure 2. Calculated average local ionization energy on the 0.001 au surface of the (5,5) SWCNT of $C_{70}H_{20}$ having a Stone-Wales defect (**1**). Two sides of the tube are shown: (a) the side with the Stone-Wales defect; (b) the side opposite the Stone-Wales defect. Color ranges, in eV: purple, less than 13.3; blue, between 13.3 and 13.5; green, between 13.5 and 14.0; yellow, between 14.0 and 14.7; red, greater than 14.7. Both the highest and the lowest $\bar{I}_s(\mathbf{r})$ are in the defect region.

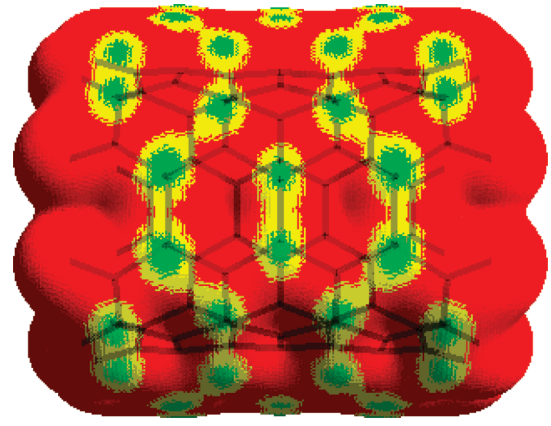

Figure 3. Calculated average local ionization energy on the 0.001 au surface of the defect-free (5,5) SWCNT of $C_{70}H_{20}$ (**2**). Color ranges, in eV: green, between 13.5 and 14.0; yellow, between 14.0 and 14.7; red, greater than 14.7.

Table 1. Computed Properties at Various Carbon Sites of (5,5) Stone-Wales Defect Nanotube **1** and Defect-Free Tube **2**[a]

				H atom chemisorption		F atom chemisorption	
nanotube	C atom site for H or F chemisorption	θ_P (deg)	$\bar{I}_{S,min}$ (eV)	C−H distance (Å)	ΔE (kcal/mol)	C−F distance (Å)	ΔE (kcal/mol)
1	C2	0.3	14.62	1.110	−32.1	1.449	−41.1
	C3	7.9	13.14	1.103	−49.7	1.415	−59.4
	C4	6.4	13.32	1.107	−45.6	1.428	−56.4
	C7	4.7	13.96	1.107	−35.7	1.431	−47.4
	C8	2.5	14.03	1.107	−33.6	1.443	−45.0
	C11	4.6	13.93	1.106	−35.7	1.436	−46.2
	C12	5.5	13.74	1.108	−35.5	1.436	−47.4
	C13	6.3	13.56	1.105	−42.4	1.428	−54.5
	C14	6.5	13.45	1.103	−48.5	1.419	−59.5
2	C2	5.3	13.78	1.108	−34.3	1.436	−45.3
	C3	5.7	13.70	1.108	−35.0	1.435	−46.5
	C4	6.0	13.55	1.105	−42.8	1.427	−54.6

[a] Numbering of carbon atoms is shown in Figure 1.

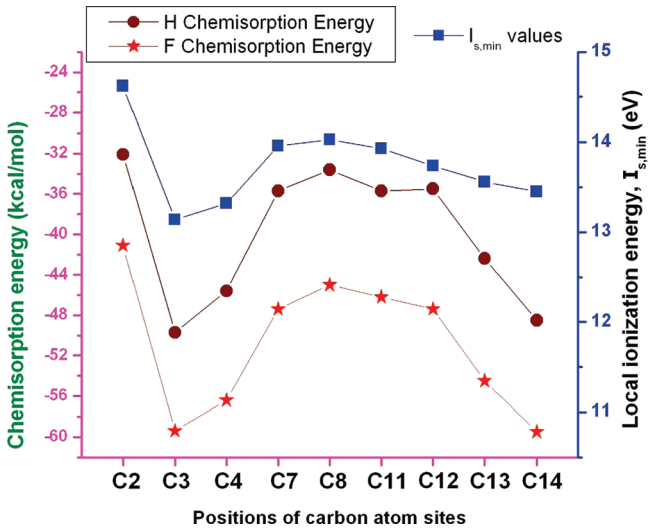

Figure 4. Variation of chemisorption energies (in kcal/mol), calculated at the UB3LYP/6-31G(d) level, for H and F atom chemisorptions at different carbon sites of Stone-Wales defective (5,5) SWCNT (**1**). Plot also shows the minimum values of the average local ionization energy ($\bar{I}_{S,min}$, in eV) at the respective carbon sites.

region are more reactive toward H and F atoms than those in the defect-free tube, while others are less reactive.

Bettinger has investigated computationally, UB3LYP/6-31G(d)//UPBE/3-21G, the reaction energies of fluorine atom additions with (5,5) SWCNTs of various lengths.[45] He found ΔE to oscillate, being most negative for the fully benzenoid systems. For our tube **2** in Figure 1, he obtained $\Delta E \approx -45$ kcal/mol, very close to our values for C2 and C3 (Table 1).

Figure 4 compares the H and F atom chemisorption energies (ΔE) at various carbon sites on the defect-containing SWCNT (**1**). The trends are very similar, but ΔE for the fluorine addition is consistently 10−12 kcal/mol larger in magnitude than hydrogen addition. Figure 4 also includes the local minima ($\bar{I}_{S,min}$) of the average local ionization energy $\bar{I}_s(\mathbf{r})$ that are associated with the respective carbon atoms. There is clearly a good correlation between the $\bar{I}_{S,min}$ and the ΔE for both the H and F chemisorptions. The lower the $\bar{I}_{S,min}$, the larger in magnitude is the chemisorption energy, i.e., the more reactive is the carbon. The only discrepancy is C14, which is more reactive in terms of ΔE than its $\bar{I}_{S,min}$would predict. $\bar{I}_{S,min}$ and the ΔE are in agreement concerning the high reactivity of C3, which is shared by five-, six-, and seven-membered rings, and the low reactivity of C2, shared by two seven-membered and one five-membered ring. Both $\bar{I}_{S,min}$ and ΔE indicate that C3 is the most reactive site and forms the strongest C−H and C−F bonds in the defect portion of the tube. Figure 5 shows the addition of H and F atoms to the most favorable site (C3) of the Stone-Wales defective tube **2**. Atom C2 received considerable theoretical attention since it is involved in the bond rotation to generate the Stone-Wales defect,[21−26] but it is the least reactive among the atoms in the defect region. Figure 4 strikingly demonstrates the general effectiveness of the average local ionization energy in predicting the relative reactivities of different sites of the Stone-Wales defective (5,5) armchair SWCNT. A single calculation deals with the entire surface of a large system, in contrast to the slower and more expensive calculations of ΔE at different sites.

Table 1 shows that the chemisorptions of H and F atoms at C7, C8, C11, and C12 of the Stone-Wales defect tube **1** have almost the same ΔE as C2 and C3 of the defect-free system **2**. The reactivity of C13 of **1** is similar to C4 of **2**, both of the carbon atom sites are near the ends of the tubes. The carbon site C14 is a special case, being near an end and also adjoining the defect; its very high reactivity is competitive with that of C3, as already pointed out.

A useful means of characterizing nanotube sites is in terms of their pyramidalization angles, θ_P.[15,19,25,63] This is the angle between the bonds of a given carbon to its three neighbors and the plane defined by those neighbors. The larger is θ_P at a given site, the greater is the degree of curvature there. Table 1 also lists the θ_P corresponding to various sites of **1** and **2**, calculated with Haddon's code POAVIT.[64] The carbon atom sites of the Stone-Wales defect region of **1** have a range of θ_P; C2 and C3 possess the lowest and the highest θ_P, respectively. The values of θ_P for the defect-free tube are intermediate. There are approximate correlations among θ_P, ΔE, and $\bar{I}_{S,min}$. In general, the greater is θ_P, which means the higher the degree of curvature, the greater is the reactivity, for both the Stone-Wales defective and defect-free SWCNTs.

Table 2 provides the energies of the highest-occupied and lowest-unoccupied molecular orbitals (HOMO and LUMO) of **1** and **2**, both bare and with chemisorbed H and F atoms. The HOMO−LUMO energy gaps ($E_{LUMO} - E_{HOMO}$) and the

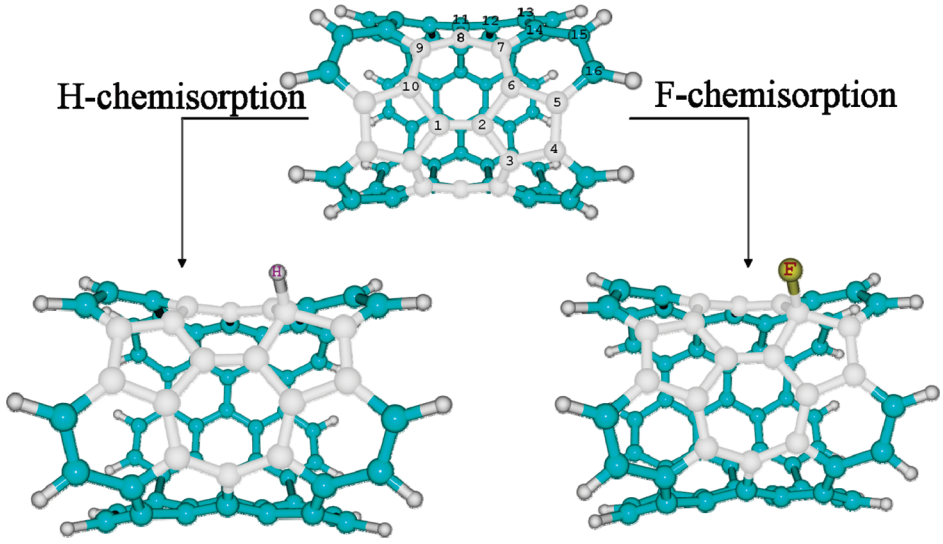

Figure 5. H- and F-chemisorbed Stone-Wales defective SWCNTs obtained by chemisorption of H and F atoms to the most favorable site (C3) in the defect region.

Table 2. Computed Properties of Bare (5,5) Carbon Nanotubes **1** (with Stone-Wales defect) and **2** (defect-free) as well as the Same Tubes with H and F Atom Chemisorbed at Sites Indicated[a]

		H atom chemisorption				F atom chemisorption			
nanotube	C atom site for H or F chemisorption	HOMO (eV)	LUMO (eV)	H−L gap (eV)	ν_{C-H} (cm^{-1})	HOMO (eV)	LUMO (eV)	H−L gap (eV)	ν_{C-F} (cm^{-1})
bare **1**		−4.54	−2.49	2.05		−4.54	−2.49	2.05	
1	C2	−4.47	−2.86	1.61	2887	−4.57	−3.19	1.37	881
	C3	−4.54	−2.64	1.90	2981	−4.65	−2.84	1.81	1039
	C4	−4.60	−2.71	1.88	2935	−4.74	−2.95	1.79	993
	C7	−4.64	−2.90	1.74	2921	−4.84	−3.25	1.59	973
	C8	−4.47	−2.65	1.81	2910	−4.54	−3.08	1.46	946
	C11	−4.53	−2.74	1.79	2924	−4.61	−3.19	1.42	965
	C12	−4.63	−2.63	1.99	2903	−4.76	−3.01	1.75	966
	C13	−4.67	−2.75	1.92	2944	−4.80	−3.08	1.73	986
	C14	−4.69	−2.79	1.90	2981	−4.82	−3.01	1.80	1029
bare **2**		−4.51	−2.30	2.21		−4.51	−2.30	2.21	
2	C2	−4.47	−2.77	1.70	2908	−4.56	−3.25	1.32	972
	C3	−4.65	−2.66	1.99	2907	−4.83	−3.09	1.74	968
	C4	−4.67	−2.79	1.88	2949	−4.81	−3.11	1.70	992

[a] Numbering of atoms is shown in Figure 1.

C−H and C−F stretching frequencies ν_{C-H} and ν_{C-F} are also included. For a defect-free (5,5) tube with no chemisorbed species, Zhou et al. obtained HOMO and LUMO energies of −4.50 and −2.30 eV,[65] which have been reproduced in our present study for bare tube **2** (Table 2). It has been demonstrated that the HOMO−LUMO gap decreases with increasing tube length, but in an oscillatory manner.[65−67]

Modifications of SWCNTs can produce dramatic effects on electronic properties and can be exploited in the design of novel electronic devices. Therefore, it is important to understand how HOMO−LUMO energy gaps are affected by the Stone-Wales defect and the chemisorptions of H and F atoms at various carbon atom sites. Creating a Stone-Wales defect in a (5,5) SWCNT slightly decreases the HOMO−LUMO energy gap, from 2.21 to 2.05 eV, mainly because of the effect upon the LUMO energy (Table 2). For both defect and defect-free tubes, chemisorptions of H or F atoms generally change both the HOMO and the LUMO energies more negatively, especially the latter. The consequences for the HOMO−LUMO gaps are that they become smaller, particularly when fluorine atoms are chemisorbed. For the Stone-Wales defective SWCNTs, the smallest gap is observed when the H or F is chemisorbed at C2, which was found to be the least reactive site.

The C−H stretching frequencies in Table 2 are all in the 2900−3000 cm^{-1} range, which is consistent with the 2920 cm^{-1} that has been obtained experimentally.[31,68] For comparison, the C−H frequencies in noncyclic alkanes are 2840−3000 cm^{-1}, while those in cyclic alkanes and alkenes are 3000−3300 cm^{-1}.[69] The highest and the lowest C−H and C−F stretching frequencies are associated with the strongest and the weakest C−H and C−F bonds (as indicated by their ΔE); these are at C3 and C2 sites of the Stone-Wales defect system **1**, respectively.

Conclusions

We have shown that the average local ionization energy, $\bar{I}_s(\mathbf{r})$, is a good indicator of the relative reactivities of the various carbon atoms of (5,5) armchair SWCNT, both with and without a Stone-Wales defect. In the Stone-Wales defective tube, the most reactive carbon atoms are predicted by $\bar{I}_s(\mathbf{r})$

to be those shared by five-, six-, and seven-membered rings, and the least reactive sites are to be those shared by two seven- and one five-membered ring. The minimum values of $\bar{I}_s(\mathbf{r})$ correlate well with the chemisorption energies of hydrogen and fluorine atom addition at the respective carbon sites. The ΔE for fluorine addition is about 10−12 kcal/mol more negative than for the hydrogen addition at the corresponding carbon site. Our results indicate that $\bar{I}_s(\mathbf{r})$ is a rapid and inexpensive means for determining the relative reactivities of carbon atom sites of SWCNTs, a single calculation sufficing for the entire surface. The pyramidalization angle θ_P also exhibits a general relationship to site reactivity. The larger is θ_P, the greater is the local curvature and the more reactive is the carbon atom. The HOMO−LUMO energy gap is decreased by the presence of a Stone-Wales defect and by hydrogen and fluorine chemisorptions.

Various properties were investigated for the chemisorption of H and F atoms, and the results obtained for the defect-free nanotube are generally intermediate in the range obtained for the Stone-Wales defect tube. For example, some carbon atoms in the defect region are more reactive than those in the defect-free system; others are less. The properties of carbon atoms outside of the defect region tend to be similar to those in the defect-free tube. Being near the end of the tube, however, has a modifying influence.

Acknowledgment. This work has been supported by the High Performance Computational Design of Novel Materials (HPCDNM) Project funded by the Department of Defense (DoD) through the U.S. Army/Engineer Research and Development Center (Vicksburg, MS), Contract #W912HZ-06-C-0057, and by the Office of Naval Research (ONR), Grant 08PRO2615-00/N00014-08-1-0324. We thank ONR, ERDC, and Mississippi Center for Supercomputing Research (MCSR) for computational facilities.

References

(1) Saito, R.; Dresselhaus, G.; Dresselhaus, M. S. *Physical Properties of Carbon Nanotubes*; Imperial College Press: London, 1998; pp 1−261.

(2) Ajayan, P. M. *Chem. Rev.* **1999**, *99*, 1787.

(3) Harris, P. J. F. *Carbon Nanotubes and Related Structures*; Cambridge University Press: Cambridge, U. K., 1999; pp 1−283.

(4) Politzer, P.; Murray, J. S.; Lane, P.; Concha, M. C. In *Handbook of Semiconductor Nanostructures and Devices*; Balandin, A. A., King, K. L., Eds.; American Scientific Publishers: Los Angeles, 2006; Vol. 2; pp 215−240.

(5) Zhou, C.; Kong, J.; Yenilmez, E.; Dai, H. *Science* **2000**, *290*, 1552.

(6) Lee, J.; Kim, H.; Kahng, S. J.; Kim, G.; Son, Y. W.; Ihm, J.; Kato, H.; Wang, Z. W.; Okazaki, T.; Shinohara, H.; Kuk, Y. *Nature* **2002**, *415*, 1005.

(7) Yang, S. H.; Shin, W. H.; Kang, J. K. *J. Chem. Phys.* **2006**, *125*, 084705.

(8) Stone, A. J.; Wales, D. J. *Chem. Phys. Lett.* **1986**, *128*, 501.

(9) Smith, B. W.; Luzzi, D. E. *J. Appl. Phys.* **2001**, *90*, 3509.

(10) Orlikowski, D.; Nardelli, M. B.; Bernholc, J.; Roland, C. *Phys. Rev. Lett.* **1999**, *83*, 4132.

(11) Lee, S.; Kim, G.; Ki, H.; Choi, B. Y.; Lee, J.; Jeong, B. W.; Ihm, J.; Kuk, Y.; Kahng, S. J. *Phys. Rev. Lett.* **2005**, *95*, 166402.

(12) Berthe, M.; Yoshida, S.; Ebine, Y.; Kanazawa, K.; Okada, A.; Taninaka, A.; Takeuchi, O.; Fukui, N.; Shinohara, H.; Suzuki, S.; Sumitomo, K.; Kobayashi, Y.; Grandidier, B.; Stievenard, D.; Shigekawa, H. *Nano Lett.* **2007**, *7*, 3623.

(13) Crespi, V. H.; Benedick, L. X.; Cohen, M. L.; Louie, S. G. *Phys. Rev. B* **1996**, *53*, R13303.

(14) Nardelli, M. B.; Yakobson, B. I.; Bernholc, J. *Phys. Rev. B* **1998**, *57*, R4277.

(15) Eggen, B. R.; Heggie, M. I.; Jungnickel, G.; Latham, C. D.; Jones, R.; Briddon, P. R. *Science* **1996**, *272*, 87.

(16) Ewels, C. P.; Heggie, M. I.; Briddon, P. R. *Chem. Phys. Lett.* **2002**, *351*, 178.

(17) Suenaga, K.; Wakabayashi, H.; Koshino, M.; Sato, Y.; Urita, K.; Iijima, S. *Nat. Nanotechnol.* **2007**, *2*, 358.

(18) Dinadayalane, T. C.; Leszczynski, J. Toward nanomaterials: Structural, Energetic and Reactivity Aspects of Single-Walled Carbon Nanotubes. In *Nanomaterials: Design and Simulation*; Balbuena, P. B.; Seminario, J. M. Eds.; Theoretical and Computational Chemistry, Elsevier: Amsterdam, The Netherlands, 2007; Vol. 18, pp 167−199.

(19) Dinadayalane, T. C.; Leszczynski, J. *Chem. Phys. Lett.* **2007**, *434*, 86.

(20) Bettinger, H. F. *J. Phys. Chem. B* **2005**, *109*, 6922.

(21) Yong, S. H.; Shin, W. H.; Lee, J. W.; Kim, S. Y.; Woo, S. I.; Kang, J. K. *J. Phys. Chem. B* **2006**, *110*, 13941.

(22) Wang, C.; Zhou, G.; Liu, H.; Wu, J.; Qiu, Y.; Gu, B.-L.; Duan, W. *J. Phys. Chem. B* **2006**, *110*, 10266.

(23) Akdim, B.; Kar, T.; Duan, X.; Pachter, R. *Chem. Phys. Lett.* **2007**, *445*, 281.

(24) Lu, X.; Chen, Z.; Schleyer, P. v. R. *J. Am. Chem. Soc.* **2005**, *127*, 20.

(25) Andzelm, J.; Govind, N.; Maiti, A. *Chem. Phys. Lett.* **2006**, *421*, 58.

(26) Govind, N.; Andzelm, J.; Maiti, A. *IEEE Sensors J.* **2008**, *8*, 837.

(27) Robinson, J. A.; Snow, E. S.; Badescu, S. C.; Reinecke, T. L.; Perkins, F. K. *Nano Lett.* **2006**, *6*, 1747.

(28) Charlier, J.-C.; Amara, H.; Lambin, Ph. *ACS Nano* **2007**, *1*, 202.

(29) Rivera, J. L.; Rico, J. L.; Starr, F. W. *J. Phys. Chem. C* **2007**, *111*, 18899.

(30) Nikitin, A.; Ogasawara, H.; Mann, D.; Denecke, R.; Zhang, Z.; Dai, H.; Cho, K.; Nilsson, A. *Phys. Rev. Lett.* **2005**, *95*, 225507.

(31) Zhang, G.; Qi, P.; Wang, X.; Lu, Y.; Mann, D.; Li, X.; Dai, H. *J. Am. Chem. Soc.* **2006**, *128*, 6026.

(32) Stojkovic, D.; Lammert, P. E.; Crespi, V. H. *Phys. Rev. Lett.* **2007**, *99*, 026802.

(33) Yang, F. H.; Lachawiec, A. J., Jr.; Yang, R. T. *J. Phys. Chem. B* **2006**, *110*, 6236.

(34) Dinadayalane, T. C.; Kaczmarek, A.; Łukaszewicz, J.; Leszczynski, J. *J. Phys. Chem. C* **2007**, *111*, 7376.

(35) Kaczmarek, A.; Dinadayalane, T. C.; Łukaszewicz, J.; Leszczynski, J. *Int. J. Quantum Chem.* **2007**, *107*, 2211.

(36) Dinadayalane, T. C.; Leszczynski, J. Toward understanding of hydrogen storage in single-walled carbon nanotubes by chemisorption mechanism. In *Practical Aspects of Computational Chemistry: Methods, Concepts and Applications*; Leszczynski, J., Shukla, M. K., Eds.; Springer: New York, 2009; pp 297−313.

(37) Lu, G.; Scudder, H.; Kioussis, N. *Phys. Rev. B* **2003**, *68*, 205416.

(38) Chamsse dine, F.; Claves, D. *Carbon* **2008**, *46*, 957.

(39) Kawasaki, S.; Komatsu, K.; Okino, F.; Touhara, H.; Kataura, H. *Phys. Chem. Chem. Phys.* **2004**, *6*, 1769.

(40) Gu, Z.; Peng, H.; Hauge, R. H.; Smalley, R. E.; Margrave, J. L. *Nano Lett.* **2002**, *2*, 1009.

(41) Chen, Z.; Thiel, W.; Hirsch, A. *ChemPhysChem* **2003**, *4*, 93.

(42) Jaffe, R. L. *J. Phys. Chem. B* **2003**, *107*, 10378.

(43) Kudin, K. N.; Scuseria, G. E.; Yakobson, B. I. *Phys. Rev. B* **2001**, *64*, 235406.

(44) Bettinger, H. F.; Kudin, K. N.; Scuseria, G. E. *J. Am. Chem. Soc.* **2001**, *123*, 12849.

(45) Bettinger, H. F. *Org. Lett.* **2004**, *6*, 731.

(46) Sjoberg, P.; Murray, J. S.; Brinck, T.; Politzer, P. *Can. J. Chem.* **1990**, *68*, 1440.

(47) Koopmans, T. A. *Physica* **1933**, *1*, 104.

(48) Nesbet, R. K. *Adv. Chem. Phys.* **1965**, *9*, 321.

(49) Janak, J. F. *Phys. Rev. B* **1978**, *18*, 7165.

(50) Politzer, P.; Murray, J. S. The average local ionization energy: concepts and applications. In *Theoretical Aspects of Chemical Reactivity*; Toro-Labbé, A., Ed.; Theoretical and Computational Chemistry, Elsevier: Amsterdam, The Netherlands, 2007; Vol. 19, pp 119−137.

(51) Politzer, P.; Murray, J. S.; Bulat, F. A. *J. Mol. Model.* **2010**, accepted.

(52) Bader, R. F. W.; Carroll, M. T.; Cheeseman, J. R.; Chang, C. *J. Am. Chem. Soc.* **1987**, *109*, 7968.

(53) Murray, J. S.; Brinck, T.; Politzer, P. *J. Mol. Struct. (Theochem)* **1992**, *255*, 271.

(54) Politzer, P.; Abu-Awwad, F.; Murray, J. S. *Int. J. Quantum Chem.* **1998**, *69*, 607.

(55) Murray, J. S.; Abu-Awwad, F.; Politzer, P. *J. Mol. Struct. (Theochem)* **2000**, *501−502*, 241.

(56) Peralta-Inga, Z.; Murray, J. S.; Grice, M. E.; Boyd, S.; O'Connor, C. J.; Politzer, P. *J. Mol. Struct. (Theochem)* **2001**, *549*, 147.

(57) Murray, J. S.; Peralta-Inga, Z.; Politzer, P.; Ekanayake, K.; LeBreton, P. *Int. J. Quantum Chem.: Biophys. Quarterly* **2001**, *83*, 245.

(58) Politzer, P.; Murray, J. S.; Concha, M. C. *Int. J. Quantum Chem.* **2002**, *88*, 19.

(59) Politzer, P.; Murray, J. S.; Lane, P.; Concha, M. C. The Remarkable Capacities of (6,0) Carbon and Carbon/Boron/Nitrogen Model Nanotubes for Transmission of Electronic Effects. In *Molecular Materials with Specific Interactions: Modeling and Design*; Sokalski, W. A., Ed.; Challenges and Advances in Computational Chemistry and Physics, Springer: Dordrecht, The Netherlands, 2007; Vol. 4, pp 487−504.

(60) Frisch, M. J.; Trucks, G. W.; Schlegel, H. B.; Scuseria, G. E.; Robb, M. A.; Cheeseman, J. R.; Montgomery, J. A., Jr.; Vreven, T.; Kudin, K. N.; Burant, J. C.; Millam, J. M.; Iyengar, S. S.; Tomasi, J.; Barone, V.; Mennucci, B.; Cossi, M.; Scalmani, G.; Rega, N.; Petersson, G. A.; Nakatsuji, H.; Hada, M.; Ehara, M.; Toyota, K.; Fukuda, R.; Hasegawa, J.; Ishida, M.; Nakajima, T.; Honda, Y.; Kitao, O.; Nakai, H.; Klene, M.; Li, X.; Knox, J. E.; Hratchian, H. P.; Cross, J. B.; Bakken, V.; Adamo, C.; Jaramillo, J.; Gomperts, R.; Stratmann, R. E.; Yazyev, O.; Austin, A. J.; Cammi, R.; Pomelli, C.; Ochterski, J. W.; Ayala, P. Y.; Morokuma, K.; Voth, G. A.; Salvador, P.; Dannenberg, J. J.; Zakrzewski, V. G.; Dapprich, S.; Daniels, A. D.; Strain, M. C.; Farkas, O.; Malick, D. K.; Rabuck, A. D.; Raghavachari, K.; Foresman, J. B.; Ortiz, J. V.; Cui, Q.; Baboul, A. G.; Clifford, S.; Cioslowski, J.; Stefanov, B. B.; Liu, G.; Liashenko, A.; Piskorz, P.; Komaromi, I.; Martin, R. L.; Fox, D. J.; Keith, T.; Al-Laham, M. A.; Peng, C. Y.; Nanayakkara, A.; Challacombe, M.; Gill, P. M. W.; Johnson, B.; Chen, W.; Wong, M. W.; Gonzalez, C.; Pople, J. A. *Gaussian 03*, revision E.01; Gaussian, Inc.: Wallingford, CT, 2004.

(61) Sjoberg, P.; Brinck, T. HardSurf program, Ph.D. dissertation, University of New Orleans, New Orleans, LA, 1991, 1993.

(62) Lide, D. R. *Handbook of Chemistry and Physics*, 78th ed.; CRC Press: Boca Raton, FL, 1997.

(63) Haddon, R. C. *Acc. Chem. Res.* **1988**, *21*, 243.

(64) Haddon, R. C. *J. Phys. Chem. A* **2001**, *105*, 4164.

(65) Zhou, Z.; Steigerwald, M.; Hybertsen, M.; Brus, L.; Friesner, R. A. *J. Am. Chem. Soc.* **2004**, *126*, 3597.

(66) Rochefor, A.; Salahub, D. R.; Avouris, P. *J. Phys. Chem. B* **1999**, *103*, 641.

(67) Zurek, E.; Autschbach, J. *J. Am. Chem. Soc.* **2004**, *126*, 13079.

(68) Zhang, G.; Qi, P.; Wang, X.; Lu, Y.; Li, X.; Tu, R.; Bangsaruntip, S.; Mann, D.; Zhang, L.; Dai, H. *Science* **2006**, *314*, 974.

(69) Silverstein, R. M.; Bassler, G. C.; Morrill, T. C. *Spectrometric Identification of Organic Compounds*; Wiley: New York, 1991; pp 103−107.

CT900669T